IS-PORTO 2023 PROCEEDINGS

Proceedings of the 8th International Symposium on DEFORMATION CHARACTERISTICS OF GEOMATERIALS Porto, 3rd - 6th September 2023

The monotonic behaviour of a low- to medium-density chalk through in-situ and laboratory characterisation

Ken Vinck[1#], *Tingfa* Liu[2], *Richard* Jardine[1], *Stavroula* Kontoe[3], *Róisín* Buckley[4], *Byron* Byrne[5], *Ross* McAdam[6], *Pedro* Ferreira[7] and *Matthew* Coop[7]

[1] *Imperial College London, Department of Civil and Environmental Engineering, London, United Kingdom*
[2] *University of Bristol, Department of Civil Engineering, Bristol, United Kingdom*
[3] *University of Patras, Department of Civil Engineering, Patras, Greece*
[4] *University of Glasgow, School of Engineering, Glasgow, United Kingdom*
[5] *University of Oxford, Department of Engineering Science, Oxford, United Kingdom*
[6] *Ørsted Power (UK) Ltd, London, United Kingdom*
[7] *University College London, Department of Civil Environmental and Geomatic Engineering, London, United Kingdom*
[#] *Corresponding author: ken.vinck15@imperial.ac.uk*

ABSTRACT

Chalk is a highly variable cemented biomicrite limestone that can show widely different rock strengths and patterns of micro to macro fissuring and jointing, due to variations in depositional environments and local geological histories. This paper describes the characterisation of a very weak to weak, low- to medium-density chalk through in situ profiling and laboratory testing, which provided new insights into the geomaterial's mechanical behaviour. The chalk de-structures when taken to large strains, leading to remarkably high pore pressures beneath penetrating cones and degraded responses in full-displacement pressuremeter tests. Laboratory tests on carefully formed specimens explored the chalk's unstable structure and marked time-, rate- and pressure dependency. A clear hierarchy was found between profiles of peak strength with depth from Brazilian tension, drained and undrained triaxial and direct simple shear tests conducted from in-situ stress conditions. Highly instrumented triaxial tests sheared from low confining stresses indicated stiffness anisotropy and showed very brittle failure behaviour from small strains. Progressively more ductile behaviour was seen as confining pressures were raised, with failures being delayed until increasingly large strains and finally stable critical states were attained. The chalk's mainly sub-vertical jointing and micro-fissuring led to properties depending on specimen scale, with high-quality laboratory stiffness measurements significantly exceeding those obtained from in-situ geophysical testing, which far exceed the operational stiffnesses of the chalk mass. While compressive strength and stiffness appear relatively insensitive to effective stress levels, consolidation to higher pressures closes micro-fissures and reduces anisotropy. The results provided the basis for numerical analysis with advanced constitutive models that inform the interpretation of axial and lateral tests on driven piles and inform the development of new practical design methods.

Keywords: Chalk; in-situ testing; laboratory testing; monotonic behaviour.

1. Introduction

Chalk, a highly variable soft cemented biomicrite limestone, underlies large areas of North-West Europe, the Middle East and other regions, posing a series of challenges to geotechnical engineers (Mortimore 2012). Chalks with unconfined compressive strengths of several MPa can stand in moderately high coastal cliffs. However, its response to foundation loading is hard to assess reliably because of its fissuring, brittleness and sensitivity. Pile driving leads to the chalk being 'de-structured' beneath the advancing pile tips and around their shafts during driving, with thin 'putty' annuli forming around their shafts (Lord et al. 2022). All these features lead to considerable uncertainty regarding driving resistances and monotonic and cyclic, axial and lateral capacities at various ages. Moreover, recent offshore North and Baltic Sea wind energy-generating projects have demonstrated that current recommendations are insufficiently reliable to guide safe and economical driven pile design in chalk (Barbosa et al. 2017, Buckley et al. 2020).

Enabling more representative characterisation of the piles' response to monotonic and cyclic, axial and lateral, loading is critical to safe and effective design for offshore wind and other onshore or nearshore projects. This aim was advanced under the ALPACA and ALPACA Plus Joint Industry Projects (JIPs), which investigated how 41, mostly instrumented, tubular steel piles behaved under dynamic, axial and lateral, monotonic and cyclic loading at the St Nicholas-at-Wade (SNW) (Kent, UK) research site (Jardine et al. 2022).

This paper summarises key findings from advanced in situ and laboratory testing conducted for ALPACA on intact low- to medium-density SNW chalk, as reported by Vinck (2021), Vinck et al. (2022) and Liu et al. (2022a). The field work included multiple CPT soundings, pressuremeter profiling, sampled boreholes and a large sampling pit. The comprehensive laboratory programme included index and oedometer profiling and over 100 advanced tests with locally instrumented, automated

stress path triaxial equipment that investigated the intact chalk's mechanical behaviour, as well as its anisotropic and yielding characteristics in tests that ranged from relatively low in-situ stress conditions to elevated pressures imposing p_0' up to 12.8 MPa.

The testing encompassed both intact and de-structured chalk. Jardine et al. (2022) show that the monotonic and cyclic axial loading performance of piles driven in chalk is governed by the behaviour of the chalk putty formed during pile driving, as manifested after reconsolidation to long-term pile shaft effective stress conditions. However, McAdam et al. (2022) and Pedone et al. (2022) show that the piles' response to monotonic lateral loading is predominantly controlled by the brittle and fractured chalk that surrounds the putty zone. The piles' response to repetitive lateral loading is also controlled by the cyclic response of 'intact' chalk that experienced additional fracturing during pile driving.

The cyclic loading triaxial experiments conducted for ALPACA are reported separately. Ahmadi-Naghadeh et al. (2022) explore the intact chalk's cyclic loading behaviour, while Liu et al. (2022b) consider the monotonic and cyclic behaviour of puttified chalk after reconsolidation to stresses comparable to those acting around the pile shafts. Liu et al. (2023) provide further interpretation of the cyclic tests and show how they can be applied in an effective stress-based method to assess the impact of axial cyclic loading in practical pile design for chalk sites.

2. Field characterisation and in situ testing

Vinck (2021) details the stratigraphy and structure of the pure white Margate and Seaford Chalk encountered at SNW, noting only slight weathering near ground level. The Chalk classifies as CIRIA grade B3/B2 (structured, very weak to weak, low-to-medium density) over the depth of interest. Predominantly vertically oriented micro-fissures were identified with 10 to 25 mm spacings at all depths.

Typical index properties and CPTu profiles and cone push-in pressumeter results are reported by Vinck et al. (2022). Corrected cone resistances ranged from 5 to 35 MPa with higher resistances in thin, discrete flint bands. Remarkably high pore water pressures (≈4 MPa) developed at u_2 (shoulder) CPTu locations as the chalk started to de-structure; the friction sleeve data showed resistances falling to 0.05 to 1 MPa as the chalk flowed past the cone tips.

Seismic CPT tests revealed a pattern for average G_{vh} values to fall largely between 1 and 2 GPa, increasing only marginally with depth, while cross-hole G_{hh} values tended to fall slightly lower. Cone push-in pressuremeter tests, conducted and interpreted by Cambridge Insitu, showed maximum non-linear (implicitly G_{hh} mode) moduli ≈1/5th of the geophysical values as well as greatly degraded shearing resistances (Vinck et al., 2022).

Index property measurements show low-density chalk with 1.43 to 1.53 Mg/m^3 intact dry density, a 0.91 average liquidity index and a degree of saturation that increased from ≈0.85 near ground surface to ≈0.97 just above the water table and ≈1.00 below.

3. Mechanical laboratory tests

The intact monotonic laboratory testing study focused on specimens prepared from three 16m deep, Geobore-S wireline triple barrel rotary boreholes and eighteen 350 x 350 x 250mm blocks which were sampled from a 7m x 10m, 4m deep excavation. The careful block sampling mobilised, wherever possible, pre-existing fissures and (mainly horizontal) bedding planes to minimise disturbance; all visibly fractured material was avoided. Hand-tools and chainsaws were used to disconnect blocks which were preserved immediately in successive layers of foil, clingfilm and wax. Expanding polyurethane foam secured the blocks in plywood storage boxes.

3.1. Laboratory specimen preparation

Laboratory mechanical test specimens require very careful preparation in chalk. Trials revealed a need for plaster-of-Paris confining moulds and water-flush coring with a highly stable radial-arm drill to assure reliable production runs of high-quality specimens (Vinck 2021). The resulting cores were then enclosed in split aluminium moulds and machined to achieve ASTM (2019) end flatness and parallelism tolerances.

3.2. Test equipment

Triaxial testing undertaken at Imperial College involved 38 mm diameter, 76 mm high specimens in computer-controlled Bishop and Wesley stress-path cells rated to 4 MPa deviatoric stresses (q) and 750 kPa cell and back pressures. Additional experiments undertaken at University College London employed GDS systems that could apply far higher cell pressures and deviator stresses, q, up to 13 MPa to 50 mm diameter, 100 mm high specimens. Vinck (2021) and Liu et al. (2022a) summarise these equipment's functional capabilities, sensitivities, resolutions and precisions, emphasising that it was not possible to measure all strains locally in the high-pressure tests.

3.3. Triaxial testing procedures

The laboratory experiments did not attempt to reproduce chalk's complex sedimentary or post-sedimentary histories and applied instead isotropic consolidation stress paths. Accurate determination of in-situ K_0 is challenging in chalk due to its typical systems of fissures, very high stiffness and sensitivity to disturbance caused by intrusive drilling. Despite the chalk's Cretaceous age and very high yield stress ratios (YSR, see Fig. 1) a low K_o = 0.6 was assumed (after Lord *et al*. 2002) when assessing in-situ stress conditions for laboratory testing. This was combined with unit weights and in-situ pore-pressure measurements from a deep piezometer and a tensiometer located above the water table ≈25 m away from the sampling pit area. Vinck et al. (2022) and Liu et al. (2022a) list the initial mean effective stresses p_0' from which drained (CID) and undrained (CIU) triaxial compression tests were undertaken to investigate the chalk's yielding in (compressive) triaxial effective stress-space.

Specimens were saturated by back pressures (300 kPa and 900kPa in the low and high-pressure tests, respectively) until Skempton's pore pressure coefficient B reached constant values greater than 0.95, before travelling on isotropic paths at 60 kPa/hour to the p_0' target. The higher-pressure tests employed stages separated by 2-3 day pause periods that allowed volume straining associated with any excess pore pressure dissipation and creep to fall below 0.015% per day. Drained monotonic axial compression followed at a 5%/day external strain rate. Load cell and other system compliances led to the local axial strain rates falling far below the external rate until the chalk yielded.

4. 1-D and isotropic compression

Fig. 1 presents Constant Rate-of-Strain (CRS) oedometer compression curves for intact, putty and reconstituted chalk samples. The putty was formed by dynamic compaction at natural water content (Vinck et al. 2022), while the reconstituted samples were formed by grinding dried chalk and mixing it to slurry at 1.4 times the liquid limit. The intact specimen converged towards reconstituted normal compression lines (NCL*) established for samples from the same depth, giving $C_c^* = 0.18$. The putty's 1-D compression behaviour is highly time-dependent; parallel stage loaded oedometer tests on puttified chalk gave secondary compression coefficients $C_{\alpha e} = \Delta e/\Delta\log10(t) = 0.003$ over the $100 < \sigma_v' < 400$kPa range of greatest interest, and a $C_{\alpha e}/C_c = 0.06$ ratio that is remarkably high for an inorganic soil. All specimens exhibited similar unloading curves, with $C_s \approx 0.01$.

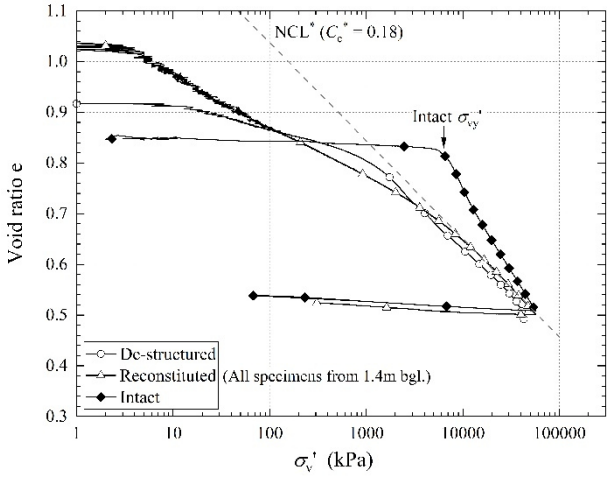

Figure 1. 1-D compression behaviour of de-structured (puttified), reconstituted and intact chalk established from CRS (constant-rate of strain; 0.6%/hour) tests

Drained probing tests by Vinck (2021) that explored the intact chalk's initial elastic behaviour revealed marked anisotropy at low pressures due to open micro-fissures, which led to far lower horizontal-than-vertical stiffnesses. However, isotropic compression to $p_0' > 350$ kPa leads to approximately isotropic stiffnesses. The chalk's isotropic compression behaviour is summarised in Fig. 2(a) by the spread of (compliance-corrected) p'-ε_{vol} data from high-pressure tests, together with the broadly compatible bulk modulus trends assessed by assuming isotropic stiffness so that $\varepsilon_{vol} = 3$ times the ε_a strains measured with (higher resolution and more accurate) local axial strain sensors in the $p_0' < 3$ MPa tests. Fig. 2(b) presents the equivalent e-log p' plot; the key points are:

- Relatively low initial $K' \approx 140$ MPa at $p' <$ 300kPa, probably due to micro-fissures (Zimmerman 1985), which appear to close tightly and allow K' to increase sharply to ≈ 2.2 GPa as pressures rise, with K' remaining steady as pressures rise until shortly before "gross" yielding led to steep K' reductions.
- In the terms proposed by Jardine (1992) and Kuwano & Jardine (2007), the end of the constant K' at $p' \approx 3$ MPa marks the point where the isotropic stress path engaged a Y_1 kinematic yield surface which bounds the space within which the behaviour was linear elastic. This yield surface is subsequently dragged with the effective stress path and may be re-entered if the path reverses or changes its direction significantly.
- The steepest rate of change in dK'/dp' applies at $p' \approx$ 3.5-4 MPa, which is interpreted (within the same framework) as a 'Y_3' yield point. The post-Y_3 section of the highest-pressure test shows how the chalk de-structures as it travels along the post-yield compression line.
- Delayed consolidation and creep straining became increasingly significant for all consolidation pause periods imposed with $p' \geq 3.2$ MPa.

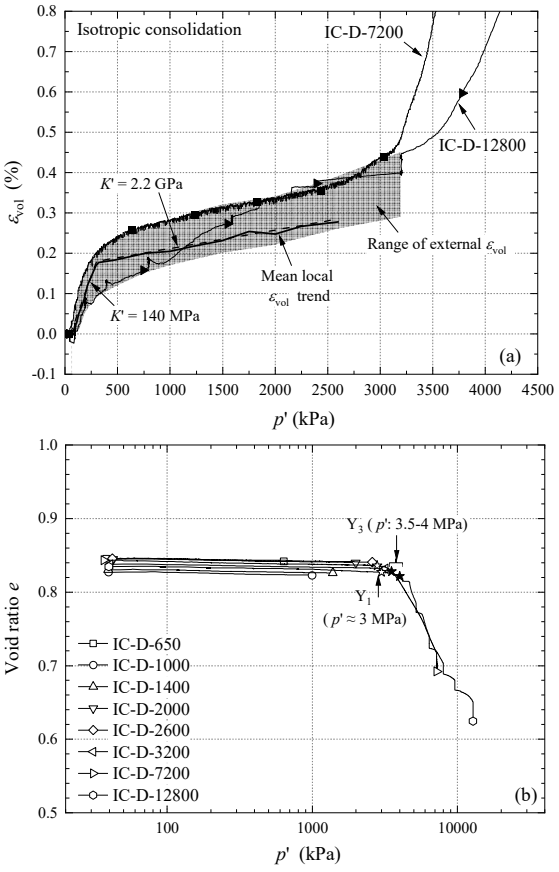

Figure 2. Intact chalk isotropic compression behaviour: (a) local and corrected external ε_{vol} against p′ and interpreted bulk stiffness trends; (b) e-p' response based on corrected ε_{vol}

5. Shearing to failure

5.1. Shear stress-strain response

Vinck et al. (2022) and Liu et al. (2022a) report a series of CID tests with p_0' ranging from 63 kPa to 12.8 MPa. Fig. 3 plots their stress-strain responses up to 0.5% axial strain. Y_1 yield points are shown to mark the ends of any initial linear portions, as are Y_3 points at the mid-points of the large-scale yielding stages where marked changes in stress-strain response occur. The experiments did not provide any systematic indication of Y_2 yielding, which was located by Jardine (1992) in clays and sands as the points where abrupt changes in strain increment directions and the development of strain rate dependency occur in drained shearing tests. These changes were interpreted as reflecting the onset of particle contact phenomena that are not expected to apply to more strongly cemented geomaterials such as chalk. The initial linear stress-strain curves condense into relatively narrow ranges up to ε_a = 0.05%. As discussed later, similar maximum values of vertical stiffnesses E_v' applied in each set, with pressure-dependent Poisson's ratios (ν_{vh}') between 0 and 0.25.

The chalk's response depended markedly on pressure. Tests p_0' < 363 kPa reached their peak strengths (q_f) at relatively small strains, with ε_a <0.1%, before fracturing and collapsing towards discontinuous assemblies of blocks and fragments. Increasing p_0' from 63kPa to 1.4 MPa led to disproportionately small increases in q_f and only a 60% gain in peak resistance. However, the degree of brittleness reduced with increasing p_0' and tests with p_0' > 2 MPa showed either a ductile or strain hardening response in terms of the effective stress ratio (q/p'). The gradual transition from brittle to ductile behaviour and illustrations of the failure patterns are detailed by Vinck et al. (2023).

The failures were markedly brittle for tests sheared from in-situ stresses, reflecting sudden losses in bond strength (or true cohesion) and the formation, or mobilisation, of discontinuities, leading to post failure states that deviated from critical states. The latter were only reached with increasing confining pressures under which intact chalk became progressively more ductile and converged towards critical states with $(q/p')_{ult} \approx 1.25$ (equivalent to $\phi_{cs}' \approx 31°$) (Liu et al. 2022a).

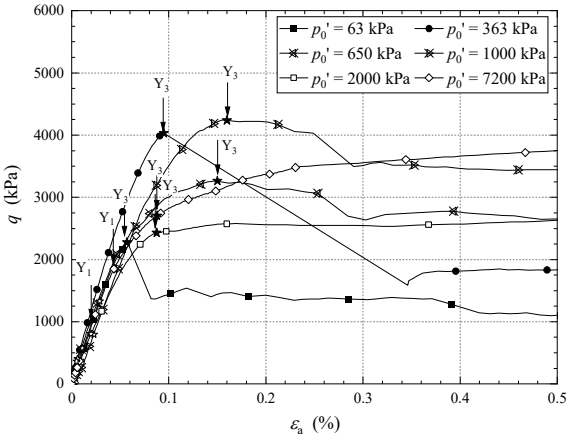

Figure 3. Typical deviatoric stress-axial strain trends over small strain range: 63 kPa < p_0' < 12.8 MPa

5.2. Volumetric strains

The shear tests' global volume and axial strain development, as presented in Fig. 4, indicate marked changes in dilatancy with increasing p_0'. Tests sheared from in-situ stresses developed minor contractive (positive) volumetric strains (≈ 0.07%) up to their peak strengths, followed by marked 'dilation' as specimens bifurcated and cracked. Similar patterns were reflected in parallel undrained tests' pore pressures (Vinck et al., 2022). Tests with 650 kPa < p_0' < 1.4 MPa exhibited (positive) volumetric strains, following a broad pattern of void ratio reductions increasing with confining pressures, reaching 6% contractive straining after 35% axial strain in the p_0' = 1.4 MPa experiment. The volumetric compressions of tests with 1.4 MPa < p_0' < 12.8 MPa appeared to condense into a narrower range that tended towards volumetric strains of 12-14%. Liu et al. (2022a) further describe the decomposition of the total strains and summarise the plastic axial and volumetric strains as proportions of the corresponding total strains ($\varepsilon_a^p/\varepsilon_a^t$, $\varepsilon_{vol}^p/\varepsilon_{vol}^t$), considering the conditions applying at the Y_3 yield points.

Elastic axial straining dominated up to Y_3 yielding in the tests sheared from in-situ stresses. However, dilative plastic volumetric strains were evident from the earliest stages of shearing. This feature probably reflects the systems of partially open micro-fractures and the micro-fissures' closure under higher pressures suppresses this apparently dilative trend, as is common with rocks; Cerfontaine & Collin (2018). The plastic strain components are more important in the higher-pressure tests where they make up, on average, around 42% and 80% of the total axial and volumetric strains at the points of Y_3 yielding, becoming dominant beyond these points.

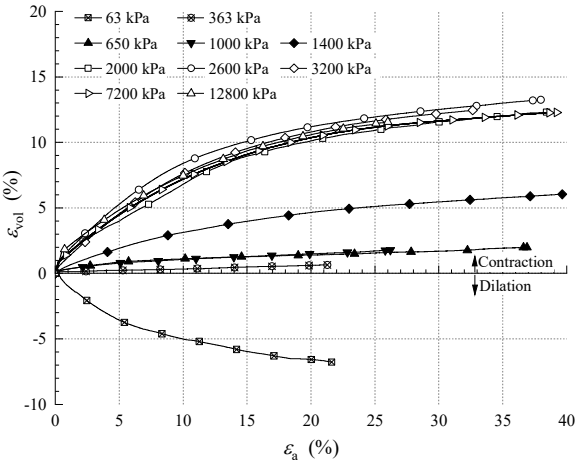

Figure 4. Volumetric strain evolution trends over full axial strain range

The corresponding q/p' - $d\varepsilon_{vol}/d\varepsilon_s$ stress-dilatancy relationships are plotted in Fig. 5. Also shown are the Y_1 and Y_3 yield points. No distinct change in the traces' curvature between these points is observed that might signify any possible, intermediate, Y_2 form of yielding. The lowest pressure, p_0' = 63 kPa, test showed dilatancy from an early stage of shearing, reflecting its open micro-fissures. Elevating pressures to p_0' > 650 kPa closed the fissures and changes altered the pre-Y_1 strain increment directions. The greater scatter seen in the early stages of

tests with $p_0' > 1.4$ MPa reflect their lack of local strain measurements, which was noted earlier.

Average Poisson's ratios ν_{vh}' of 0.25, 0.20 and 0 were interpreted for the respective suits of tests effective stress ranges. Overall, the chalk's stress-dilatancy characteristics resemble those shown by comparably weak calcarenites (Cuccovillo & Coop 1999).

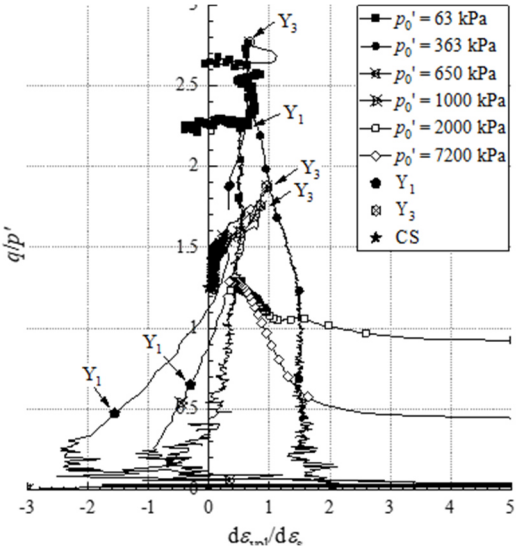

Figure 5. Stress dilatancy correlation of intact chalk

5.3. State paths during shearing

The triaxial effective stress paths presented in Fig. 6 show peak q/p' ratios close to 3, the maximum that can be applied without the minor principal effective stress going into tension. CID triaxial tests showed marked 'dilation' as the specimens cracked and bifurcated. Similar patterns were reflected in CIU tests, which showed strong pore pressure reductions as the samples failed and fractures tried to open.

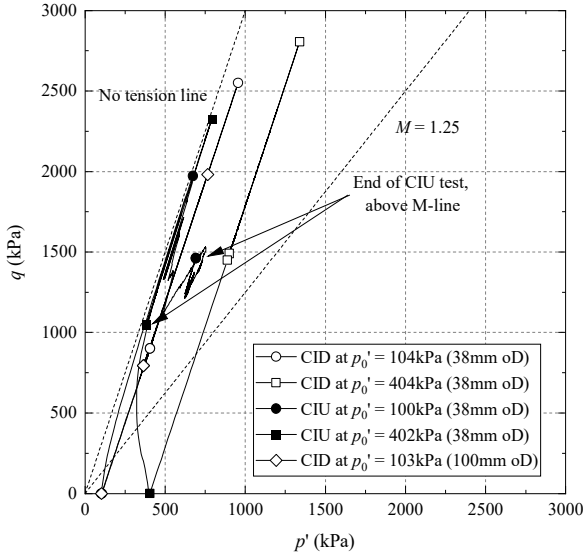

Figure 6. Effective stress paths of drained and undrained triaxial tests from isotropic conditions

The CIU tests' pre-failure effective stress paths also approached the no-tension limit, following paths with initial gradients dp'/dq between 0.16 and 0.20, which curved to the right as the tests progressed towards gradients close to the applied total stress $dp/dq = 1/3$ ratio. The initial shear-induced pore pressure ratios $A = du/dq$ (Skempton 1954) fall around half the 1/3 ratio (equivalent to $dp'/dq = 0$) expected for an isotropic elastic soil undergoing undrained compression.

Cross-anisotropic elastic theory predicts $A < 1/3$ when horizontal stiffness is less than vertical ($E_h'/E_v' < 1$) (Kuwano and Jardine 2007). The chalk's elastic stiffness anisotropy, which is explored further in later sections, is interpreted as the main reason for the low initial A values. CIU tests conducted after consolidation to higher p_0' gave more vertical q-p' paths and A values compatible with $E_h' \approx E_v'$.

5.4. Peak shear strength

The chalk's peak strength envelope is curved, leading to shear strength parameters that vary markedly with pressure. Vinck *et al*. (2022) adopted a pressure-dependent Mohr-Coulomb model to distinguish broadly how intact chalk's 'bonded' and 'frictional' components of strength varied with pressure level. They combined CID and CIU triaxial tests covering 63 kPa < p_0' < 450 kPa to interpret a representative intact peak Mohr-Coulomb envelope with a $c' = 490$ kPa and $\phi_{peak}' = 39.6°$ which is re-plotted in Fig. 7; other fits apply over different pressure ranges. The lowest p_0' tests developed peak strengths situated marginally to the right of the $\sigma_3' = 0$ and $q/p' = 3$ (no tension) limit that applies in all triaxial tests. The 'low-pressure' tests' relatively high apparent cohesion component reflects the level of inter-particle bonding between the cemented silt-sized calcium carbonate ($CaCO_3$) aggregates, but it is not synonymous with the true component of bonded shear strength, which could not be identified directly from the Authors' experiments.

Increasing p_0' clearly weakens inter-grain bonding and promotes a more 'frictional' shearing response with a curved yield envelope with $M \approx 1.25$ or $\phi_{cs}' \approx 31°$ at critical state, implying pressure dependent c' and ϕ_{peak}' for dry of critical conditions.

While variations between specimens led to a range of low-pressure brittle bifurcation failure patterns, most tended to form shear zones inclined at 60-65° to the horizontal. The 'high pressure' ductile specimens formed bulging failures and delivered markedly reduced post-test water contents (16-23%), while 'elevated pressure' specimens developed both radial bulging and formed 6-8 mm thick bands of remoulded chalk within diffused shear zones inclined ≈65° to the horizontal.

The peak triaxial compressive shear strengths of bonded weak rocks are relatively insensitive to consolidation paths applied within their Y_3 envelopes (Leroueil & Vaughan 1990). They generally offer far lower strengths in tension. Vinck et al. (2022) confirm that far lower shear strengths and stiffness apply to chalk in tests that induce tensile failure. Their Brazilian tension strengths were 90% lower than the UCS values, while the direct simple shear (DSS) strengths were 50% lower than those mobilised in triaxial compression.

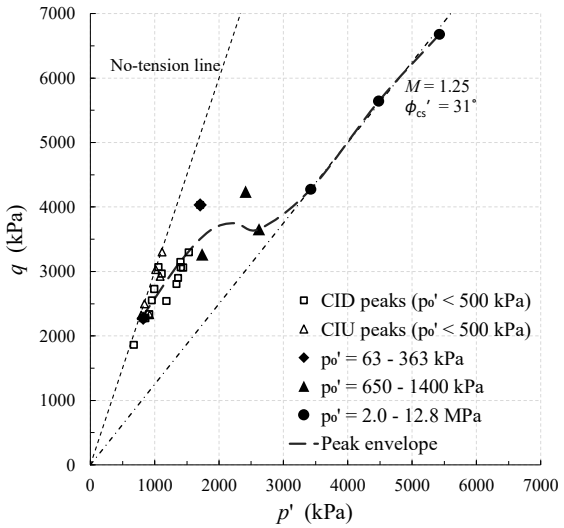

Figure 7. Peak and ultimate shear strength envelope for intact chalk

5.5. Stiffness behaviour prior Y_3 yielding

All shearing tests presented linear initial q-ε_a sections up to the Y_1 yield points. Y_1 yielding was located where the stress-strain (q-ε_a) response deviated from the initial linear elastic trend. Linear regression of the pre-Y_1 trends led to the initial plateau in the equivalent secant E_v'-ε_a curves in Fig. 8. The linear-elastic plateaux span much large strain ranges than are commonly observed for sands and clays. Specimens sheared from in-situ stresses exhibited mild stiffness non-linearity, with E_v' remaining largely > 4 GPa at Y_3 yielding. The degree of non-linearity increases markedly with p_0' with smooth and continuous stiffness degradation trends observed at high pressures as they developed ductile responses towards large strains.

Kuwano & Jardine (2007) and Ushev & Jardine (2020) show that unbonded sands, clays and silt-dominated tills generally display small Y_1 kinematic yield loci, which often extend for just a few kPa in q-p' space. In contrast, the chalk displays linear behaviour over a remarkably large region of q-p' space. Furthermore, as shown in Fig. 9, the $E_{v,max}'$ maxima show relatively modest (< 50%) gains after a tenfold increase in p_0' from in-situ levels to 650 kPa before $E_{v,max}'$ falls to a lower limit ≈ 4 GPa that is maintained until p_0' > 4 MPa. Vinck (2021) shows that the Y_1 surface can be relocated and potentially modified by imposing sufficiently large (drained or undrained) changes in q, followed by pause periods in which creep straining is allowed to reduce to slow rates.

Overall, the intact chalk's small strain stiffness behaviour appears to be controlled by both its initially cemented particulate structure and its systems of micro-to-macro fissures. The cemented contacts appear to be damaged by high-pressure anisotropic loading as shearing progresses between the Y_1 and Y_3 yield points identified in Fig. 8 and undergo still greater damage after isotropic loading to high p'. The destructured chalk's stiffness gradually tends towards that expected for unbonded silts or fine sands at similar states, as noted for calcarenite, sandstone and other cemented soils tested at high confining pressures (Cuccovillo & Coop 1997).

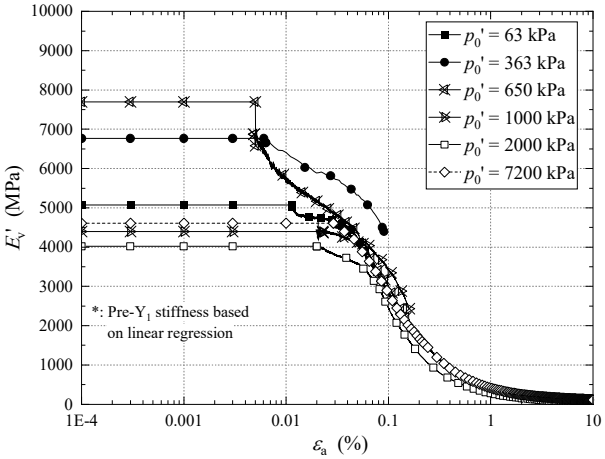

Figure 8. Degradation trends of vertical drained secant Young's modulus

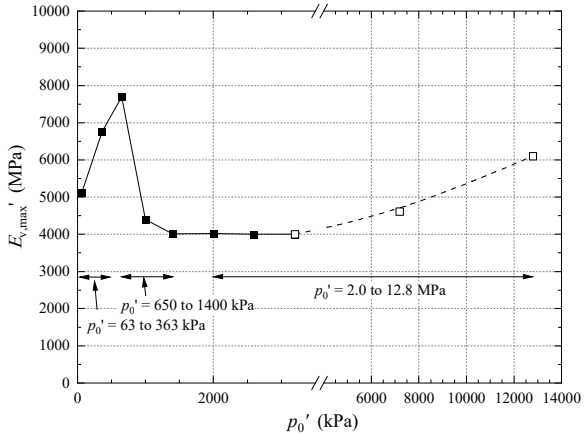

Figure 9. Variations of maximum vertical drained Young's moduli ($E_{v,max}'$) against p_0'

5.6. Stiffness anisotropy

The CIU tests' effective stress path inclinations and the systematic trend for initial E_v' to exceed E_v^u indicated that the chalk's vertical moduli exceed equivalent horizontal stiffnesses under in-situ stress conditions. Vinck (2021) explored the anisotropy more precisely in his Series E tests through high-resolution BE and monotonic stress probing experiments. Figure 10 presents the profiles with depth of the G_{hh}/G_{vh} ratios found from field and laboratory tests. Dual axis triaxial BE measurements, made on the same samples, gave G_{hh}/G_{vh} ≈0.5 in the shallow layers and ratios exceeding unity at depth. The G_{hh}/G_{vh} ratios from field seismic tests show a similar, but more muted, trend.

Vinck (2021) also applied small-strain axial and radial drained probes to his triaxial specimens to assess whether their stress-strain behaviour was linear, recoverable, and potentially anisotropic within any Y_1 kinematic yield surface. The vertical stiffnesses were found easily from the high-resolution axial stress and strain measurements. Horizontal stiffness assessment is less direct. Kuwano and Jardine (2002) give alternative routes for deriving full sets of cross-anisotropic compliance parameters from combined radial probing tests, which define the parameter R in Eq. (1) below and BE G_{hh} measurements. However, even small radial increments applied from in-situ stresses led to responses

that were hysteretic and non-uniform around the samples' perimeters, reflecting the presence of imperfectly closed, mainly vertical, micro-fissures. In some cases, treating the chalk as an elastic continuum led to implausible cross-anisotropic v_{hv}' ratios because the samples' radial behaviour was neither continuous nor fully recoverable, even at very small strains. Vinck (2021) shows that Eqs. (1) and (2) provide the most robust assessments of horizontal stiffness $E_{h,max}'$, where under axisymmetric triaxial conditions:

$$R = \Delta\sigma_h'/\Delta\varepsilon_h \quad (1)$$

$$E_h' = \frac{4\,R\,G_{hh}}{R+2\,G_{hh}} \quad (2)$$

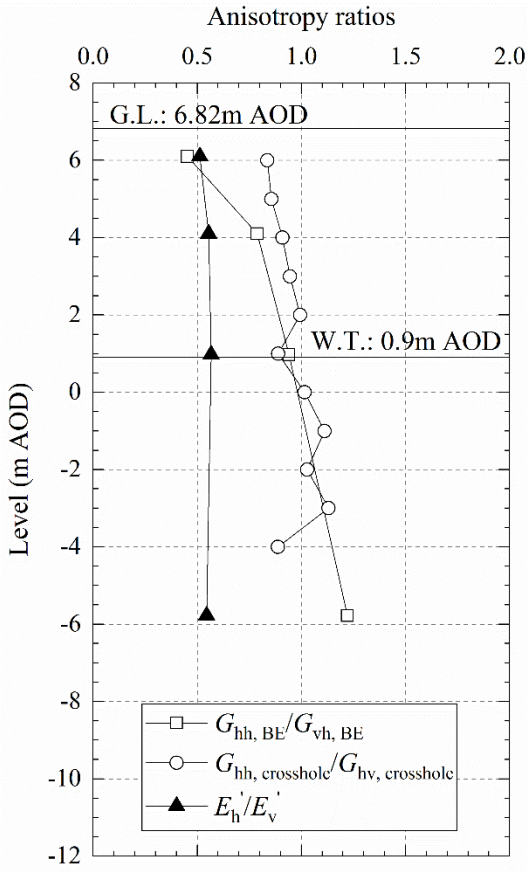

Figure 10. Profiles of stiffness anisotropy as obtained from bender measurements and cross-hole investigations and suites of drained and undrained triaxial probing

The E_h'/E_v' profile in Fig. 10 derived from probing tests confirms that horizontal loading from in-situ stresses provokes a far softer response than vertical compression, which is critically important when analysing lateral pile loading. Vinck (2021) shows that anisotropy diminishes after consolidation to higher pressures.

It is vitally important to emphasise that the elastic stiffnesses interpreted from the ALPACA pile tests fell far below those indicated by the field geophysics or laboratory element tests on intact samples. Jardine et al. (2022) and Pedone et al. (2022) conclude that this is due to the systems of meso-to-macro fissures which are present in the chalk mass but are systematically avoided in the preparation of test specimens and can be by-passed by geophysical body waves.

6. Conclusions

This paper summarises the key outcomes from comprehensive in-situ and laboratory testing on intact low- to medium-density chalk conducted for the ALPACA JIPs to aid the interpretation of axial and lateral pile load tests. The key conclusions drawn are:

1. Intact chalk exists at states it cannot sustain when reconstituted. It is highly sensitive and de-structures when taken to large strains.
2. De-structuration and tensile failure affect the responses seen in field and laboratory shear tests.
3. A clear hierarchy exists between strengths obtained from UCS, triaxial, DSS and BT tests.
4. The chalk's behaviour is markedly pressure dependent. When loaded from in-situ p_0' conditions, it manifests remarkably brittle, bonded behaviour after relatively small axial strains (≈0.15%) with apparent cohesion components that contribute a large proportion of their peak deviator stresses. However, this decays rapidly post-peak.
5. Raising the initial isotropic p_0' levels into the MPa range leads to ductile behaviour and compressive volumetric straining. All experiments conducted with $p_0' \geq 650$ kPa tended towards final critical states with $M = 1.25$, equivalent to $\phi' \approx 31°$.
6. Specimen failure patterns also evolve from showing discontinuous bifurcation after small axial strains (≈ 0.1%) to bulging and peak resistances developing after large (≈ 40%) strains.
7. Drained isotropic loading invokes tangent bulk moduli K′ that initially increase until micro-fissures close fully, after which K′ remains high and practically constant until large strain yielding commences and sharp K′ reductions occur.
8. The chalk also shows very stiff initial near linear shearing behaviour. Vertical Young's moduli E_v' increase modestly with pressure until they manifest their maximum (7.7 GPa) at moderate pressures (with $p_0' = 650$ kPa) before falling to a 4 MPa minimum plateau. This behaviour differs strikingly from that of unbonded geomaterials.
9. CID and CIU triaxial compression tests sheared from in situ stresses developed closely similar effective stress paths inclinations reflecting marked stiffness anisotropy, with $E_h'/E_v' < 1$ due to open micro-fissures. Samples consolidated to pressures that close these fissures show far less anisotropy. Field geophysical tests reveal similar patterns for $G_{hh}'/G_{hv}' < 1$.
10. Meso-to-macro systems of fissuring lead to field axial and lateral pile loading experiments showing far lower elastic stiffnesses than either field geophysical, or locally instrumented triaxial tests on intact specimens.

Acknowledgements

The joint experimental studies between Imperial College and University College London were undertaken under the ALPACA and ALPACA Plus projects funded by the Engineering and Physical Science Research Council (EPSRC) grant EP/P033091/1, Royal Society Newton Advanced Fellowship NA160438 and Supergen ORE Hub 2018 (EPSRC EP/S000747/1). The Royal Academy of Engineering supports Prof Byrne under the Research Chairs and Senior Research Fellowships scheme. The authors acknowledge additional financial and technical support by Atkins, Cathie Associates, Equinor, Fugro, Geotechnical Consulting Group (GCG), Iberdrola, Innogy, LEMS, Ørsted, Parkwind, Siemens, TATA Steel and Vattenfall. Imperial College's EPSRC Centre for Doctoral Training (CDT) in Sustainable Civil Engineering and the DEME Group (Belgium) supported Dr Vinck. The Authors also acknowledge contributions to CPT and pressuremeter testing, block and rotary core sampling and DSS testing by Cambridge Insitu, Fugro, Lankelma and Socotec UK. Ben Boorman and Matt Wilkinson at University College London and Steve Ackerley, Graham Keefe, Prash Hirani, Stef Karapanagiotidis, Graham Nash and Gary Jones at Imperial College London are thanked for their invaluable technical support.

References

Ahmadi-Naghadeh, R., T. Liu, K. Vinck, R. J. Jardine, S. Kontoe, B. W. Byrne, R. A. McAdam. "Laboratory characterisation of the response of intact chalk to cyclic loading". Ahead of Print in Géotechnique, 2022. https://doi.org/10.1680/jgeot.21.00198

ASTM International. D4543-19: Standard Practices for Preparing Rock Core as Cylindrical Test Specimens and Verifying Conformance to Dimensional and Shape Tolerances. West Conshohocken, PA; ASTM International, 2019. https://doi.org/10.1520/D4543-19

Barbosa, P. M., M. Geduhn, R. J. Jardine, F. C. Schroeder. "Large scale offshore static pile tests-practicality and benefits". Society for Underwater Technology: 8th International Conference on Offshore Site Investigation and Geotechnics, Smarter Solutions for Offshore Developments, London, UK, vol. 1, 644-651, 2017.

Buckley, R. M., R. J. Jardine, S. Kontoe, P. Barbosa, F. C. Schroeder. "Full-scale observations of dynamic and static axial responses of offshore piles driven in chalk and tills". Géotechnique, 70(8): 657-681, 2020. https://doi.org/10.1680/jgeot.19.TI.001

Cerfontaine, B., F. Collin. "Cyclic and fatigue behaviour of rock materials: Review, interpretation and research perspectives". Rock Mech Rock Eng 51, 391–414, 2018. https://doi.org/10.1007/s00603-017-1337-5

Cuccovillo, T., M. R. Coop. "Yielding and pre-failure deformation of structured sands". Géotechnique, 47(3):491-508, 1997. https://doi.org/10.1680/geot.1997.47.3.491

Cuccovillo, T., M. R. Coop, "On the mechanics of structured sands". Géotechnique, 49(6):741-760, 1999. https://doi.org/10.1680/geot.1999.49.6.741

Jardine, R. J. "Some observations on the kinematic nature of soil stiffness". Soils and Foundations, 32(2):111-124, 1992. https://doi.org/10.3208/sandf1972.32.2_111

Jardine, R. J., R. M. Buckley, T. Liu, T. Andolfsson, B. W. Byrne, S. Kontoe, R. A. McAdam, F. Schranz, K. Vinck. "The axial behaviour of piles driven in chalk", 2022. Accepted for publication in Géotechnique.

Kuwano, R., R. J. Jardine. "On the applicability of cross-anisotropic elasticity to granular materials at very small strains". Géotechnique, 52(10):727-749, 2002. https://doi.org/10.1680/geot.2002.52.10.727

Kuwano, R., R. J. Jardine. "A triaxial investigation of kinematic yielding in sand". Géotechnique, 57(7):563-579, 2007. https://doi.org/10.1680/geot.2007.57.7.563

Leroueil, S., P. R. Vaughan. "The general and congruent effects of structure in natural soils and weak rocks". Géotechnique, 40(3):467-488, 1990.

Liu, T., P. M. V. Ferreira, K. Vinck, M. R. Coop, R. J. Jardine, S. Kontoe. "The behaviour of a low-to-medium density chalk under a wide range of pressure conditions". Accepted by Soils and Foundations, 2022a.

Liu, T., R. Ahmadi-Naghadeh, K. Vinck, R. J. Jardine, S. Kontoe, R. M. Buckley, B. W. Byrne. "An experimental investigation into the behaviour of de-structured chalk under cyclic loading". Ahead of Print in Géotechnique, 2022b. https://doi.org/10.1680/jgeot.21.00199

Liu, T., R. J. Jardine, K. Vinck, R. Ahmadi-Naghadeh, S. Kontoe, R. M. Buckley, B. W. Byrne, R. A McAdam. "Cyclic characterisation of low-to-medium density chalk for offshore driven pile design". Submitted to Offshore Site Investigation and Geotechnics Conference, Society of Underwater Technology, London, UK, 2023. https://doi.org/10.1680/geot.1990.40.3.467

Lord, J. A., C. R. L. Clayton, R. N. Mortimore. "Engineering in chalk", CIRIA, C574, 2002.

McAdam, R. A., R. M. Buckley, F. Schranz, B. W. Byrne, R. J. Jardine, S. Kontoe, T. Liu, K. Vinck, Crispin, J. "Monotonic and cyclic lateral loading of piles in low to medium density chalk", 2022. Under review.

Mortimore, R. N. "The 11th Glossop Lecture: Making sense of chalk: a total-rock approach to its engineering geology". Q. J. Engng Geol. Hydrogeol. 45, No. 3, 252–334, 2012. https://doi.org/10.1144/1470-9236/11-052.

Pedone, G., S. Kontoe, L. Zdravković, R. J. Jardine, K. Vinck, T. Liu. "Numerical modelling of laterally loaded piles driven in low-to-medium density fractured chalk". Accepted for publication by Computers and Geotechnics subject to minor revisions, 2022.

Skempton, A.W. "The Pore-Pressure Coefficients A and B". Géotechnique. 4 (4):143-147, 1954. https://doi.org/10.1680/geot.1954.4.4.143

Ushev, E. R, R. J. Jardine. "The behaviour of Bolders Bank glacial till under undrained cyclic loading". Géotechnique, 72(1):1-19, 2020. https://doi.org/10.1680/jgeot.18.P.236

Vinck, K. "Advanced geotechnical characterisation to support driven pile design at chalk sites", PhD Thesis, Imperial College London, 2021.

Vinck, K., T. Liu, R. J. Jardine, S. Kontoe, R. Ahmadi-Naghadeh, R. M. Buckley, B. W. Byrne, J. A. Lawrence, R. A. McAdam, F. Schranz. "Advanced in situ and laboratory characterisation of the ALPACA chalk research site". Ahead of Print in Géotechnique, 2022. https://doi.org/10.1680/jgeot.21.00197

Vinck, K., T. Liu, R. J. Jardine, S. Kontoe, R. M. Buckley, B. W. Byrne, R. A. McAdam, P. M. V. Ferreira, M. Coop. "Monotonic characterisation of low-to-medium density chalk for offshore driven pile design". Submitted to Offshore Site Investigation and Geotechnics Conference, Society of Underwater Technology, London, UK, 2023.

Zimmerman, R. W. "The effect of microcracks on the elastic moduli of brittle materials". Journal of Materials Science Letters, 4:1457-1460, 1985. https://doi.org/10.1007/BF00721363